LBNL-42491

ERNEST ORLANDO LAWRENCE
BERKELEY NATIONAL LABORATORY

Photodissociation of NO_2 near 225 nm by Velocity Map Imaging

M. Ahmed, D.S. Peterka, and A.G. Suits

Chemical Sciences Division

October 1998

Presented at the
21st International
Symposium on
Rarefied Gas Dynamics,
Marseille, France,
July 26–31, 1998,
and to be published in
the Proceedings

LBNL-42491

Photodissociation of NO_2 near 225 nm by Velocity Map Imaging

M. Ahmed, D.S. Peterka, and A.G. Suits

Chemical Sciences Division
Ernest Orlando Lawrence Berkeley National Laboratory
University of California
Berkeley, California 94720

October 1998

This work was supported by the Director, Office of Energy Research, Office of Basic Energy Sciences, Chemical Sciences Division, of the U.S. Department of Energy under Contract No. DE-AC03-76SF00098.

Photodissociation of NO_2 near 225 nm by Velocity Map Imaging

M. Ahmed, D. S. Peterka, A. G. Suits
Chemical Sciences Division
Ernest Orlando Lawrence Berkeley National Laboratory
Berkeley, California 94720, USA

1 Introduction

Since the pioneering work of Busch and Wilson[1] with the inception of Photofragment Translational Energy Spectroscopy (PTS), NO_2 has been one of the most studied molecules in the field of photodissociation dynamics. Recently experimentalists have been using a variety of elegant techniques to unravel the intricate photodissociation dynamics of this model triatomic molecule[2, 3]. A whole body of work has concentrated around the threshold regime (355 nm) for the $O(^3P_j)$ + NO channel. Photodissociation studies beyond the threshold regime have been sparse. These have focussed on recording the internal state distribution of the nascent NO fragment from photolysis at 248 nm utilizing laser-induced fluorescence (LIF)[4] and resonance enhanced multiphoton ionization (REMPI)[5], and photolysis around 226 nm with detection by REMPI[6]. There have also been two reports[7, 8] on the fine- structure population distributions of the oxygen atom produced by photolysis over a range of UV wavelengths. Miyawaki et al. also reported the kinetic energy of the oxygen fragment to be 0.13 eV from analysis of their Doppler profiles and that the energy release did not vary with the photolysis wavelength (355, 337, 266, and 212 nm). Shafer et al.[9] recorded the Doppler spectra for the excited oxygen atom $O(^1D)$ at 205.47 nm and derived a translational energy release which was between 0.11 eV and 0.211 eV, and an anisotropy parameter β of 1.3.

In this paper we present a study of the photodissociation dynamics for NO_2 in the region of 221-226 nm using velocity map imaging[10] (VELMI) in conjunction with REMPI. We chose this region because it allowed us to use a single laser to photodissociate and probe the NO and $O(^3P)$ products using REMPI. Probing the angular and energy distributions of both fragments under state resolved conditions allows for detailed investigations of the product state distributions in the photodissociation dynamics of NO_2.

2 Experimental

The molecular beams apparatus has been described in detail in a recent publication[11]. A 5% mixture of NO_2/O_2 seeded in He was expanded through a Proch-Trickl pulsed valve[12], collimated by a single skimmer and then crossed by a laser beam on the axis of a velocity focusing time-of-flight mass spectrometer. The photolysis and probe light around 221-226 nm was generated by doubling the output of a seeded Nd-YAG pumped dye laser in β- barium borate (BBO), then mixing the resultant UV light with the dye fundamental in a second BBO crystal.

The NO product from NO_2 dissociation was probed using (1+1) REMPI through the $A(^2\Sigma) \leftarrow X(^2\Pi)$ transition (the γ bands). The various spin-orbit states of the O product were probed using (2+1) REMPI through the $3p(^3P_J) \leftarrow\leftarrow 2p(^3P_J)$ transition.

The NO^+ and O^+ ions were accelerated toward a 80-mm diameter dual microchannel plate (MCP) coupled to a phosphor screen and imaged on a fast scan charge-coupled device camera with a integrating video recorder (Data Design AC-101M). Camera threshold and gain were adjusted in conjunction with a binary video look-up table to perform integration of single ion hits on the MCP free of video noise. Images were accumulated while scanning across the Doppler profile of the O atom, since the line width of the laser light was narrower than the Doppler spread. The translational energy and angular distributions were determined from the images by applying the inverse Abel transform and integrating appropriately.

3 Results

Fig.1 shows the raw ion-image for the $(^3P_0)$ state of the oxygen atom obtained from photodissociation of NO_2 at 226.23 nm. Similar images were obtained for the $(^3P_2)$ and $(^3P_1)$ spin orbit states of ground state oxygen but there is evidence of atomic orbital alignment for these states[13], which is the subject of a separate study. For those levels, unknown contributions of the orbital alignment can interfere with a direct determination of the anisotropy parameter. For the $(^3P_0)$ state this is not a problem, since there is no total angular momentum and hence no orbital alignment. The shape of the image in Fig.1 is from the photofragment angular distribution (the velocity anisotropy), characterized by the β parameter, which is determined to be 1.32 from the fit shown in Fig.2(B).

Examining the translational energy distributions of the oxygen atom provides a mapping of the internal state distributions of the NO cofragment because of momentum conservation. Fig.2(A) shows such a translational energy distribution for the $O(^3P_0)$ fragment. At 226.23 nm the photon energy

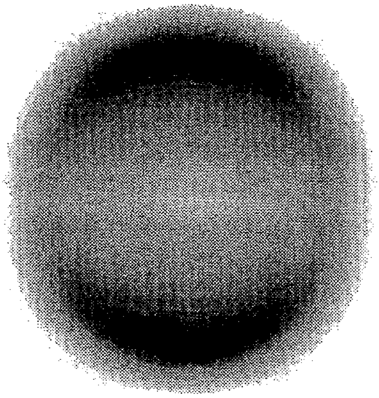

Figure 1: Image of O($^3P_0$) from NO_2 dissociation at 226.23 nm

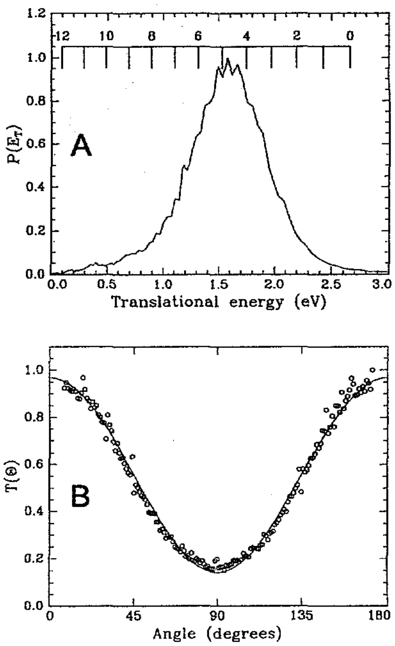

Figure 2: Translational energy (A) and angular distribution (B) of O($^3P_0$) derived from the image in the previous figure.

is 5.48 eV. The bond dissociation energy (D_0) for the $NO_2 \rightarrow NO(X^2\Pi) + O(^3P_0)$ channel is 3.11 eV. Internally cold products should show up at 2.37 eV, but the peak in Fig.2A is shifted away from this value. The main peak around 1.6 eV corresponds to a range of excited vibrational levels of the NO (X $^2\Pi$) ground state, peaking at v=4 or 5. The comb above the translational energy distribution in Fig.2 (A) shows thresholds for indicated vibrational levels in the NO cofragment. Except for v=0, the vibrational distribution for NO obtained from the O($^3P_0$) translational energy distributions are in qualitative agreement with the results of McFarlane et al[5]. They obtained highly inverted vibrational distributions of NO peaking at v=5 from NO_2 photodissociation at 248 nm. In contrast to our results, they observed significant population of NO v=0, which could be contributions from NO in their molecular beam or from NO v=5 as discussed below.

Fig.3 shows images for various ro-vibrational states of NO. The ground vibrational state images shown in Fig.3 (A) and (B) were collected with photolysis at 225.64 and 225.68 nm respectively. The image in Fig.3(B) is from the N=16 rotational state probed on the R11, Q21 line. The outer

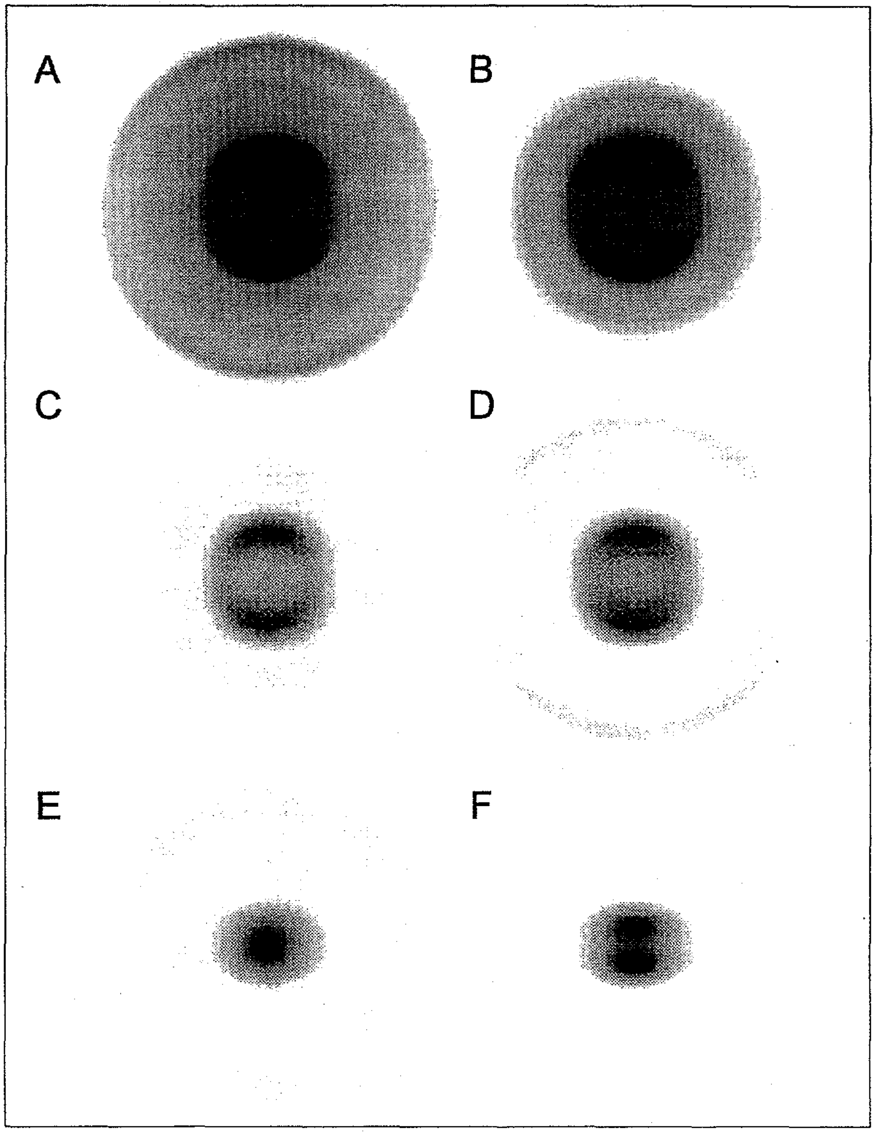

Figure 3: NO$^+$ images on various rotational lines of v=0 (A,B), v=1 (C,D) and v=2 (E,F)

ring in all the images correspond to NO formed in conjunction with O(^3P_J) and the inner ring corresponds to O(^1D). The corresponding translational energies are shown in Fig.4. At 225.64 nm (5.49 eV), for NO (v=0), O(^3P) will show up at 2.38 eV (D_0=3.11 eV) while the peak for O(^1D) will appear around 0.41 eV. This agrees very well with our experimental results as can be seen from the translational energy distributions shown in Fig4(A).

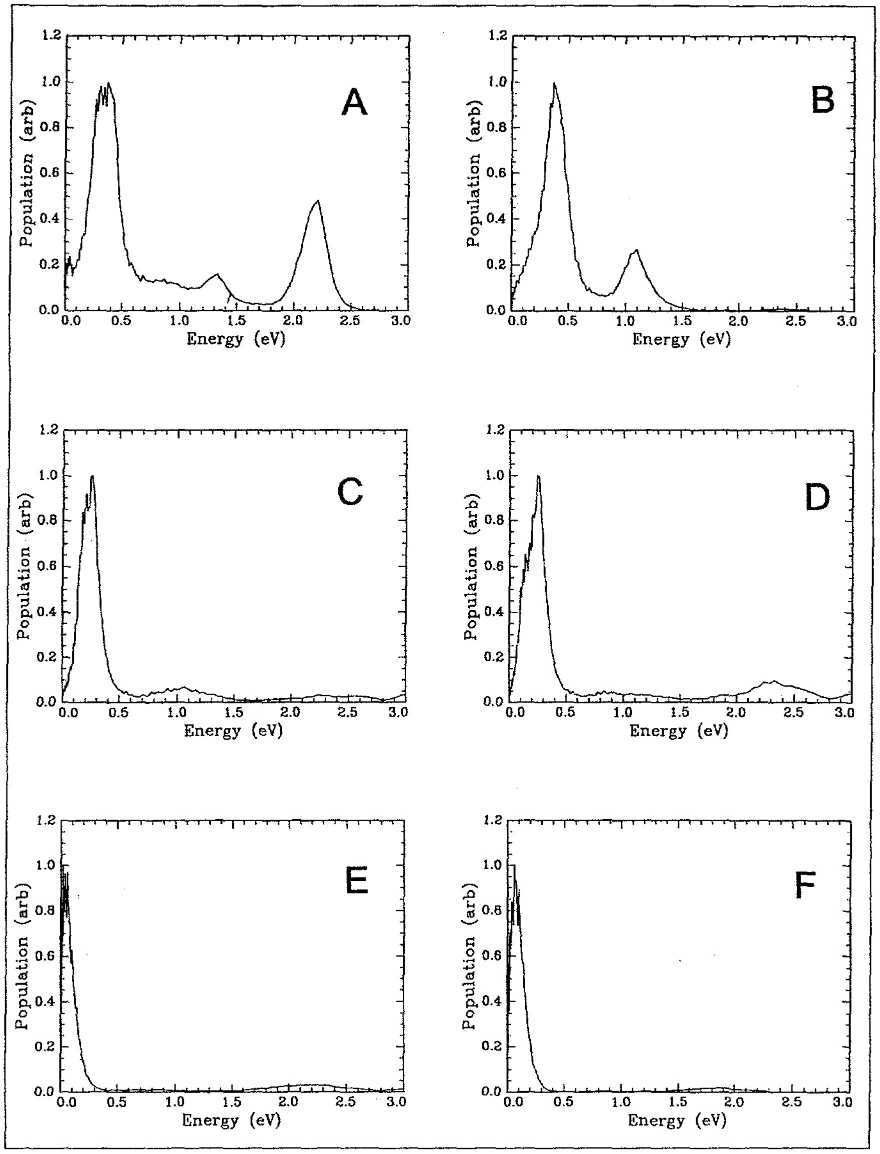

Figure 4: NO$^+$ translational energy distributions for the rotational lines of the previous figure

Comparing Fig.4(A) with Fig.4(B) shows that for very similar rotational states the branching ratio to the two oxygen atom channels are very different. For NO (v=0,N=16), the ratio for O(^1D):O(^3P) is 1:0.01 while for a nearby line it is 1:0.44. This suggests very different underlying rotational distributions for the two different channels. An alternative but perhaps less plausible explanation is a dramatic change in the dynamics with this small change in photolysis wavelength. Similar results are also seen for results for NO (v=1 and 2). In addition to the two channels mentioned above, we see a ring which is formed with a translational energy release of 1.1 eV. On energetic grounds this ring cannot arise from photodissociation of N_2O_4 (NO dimer) or from HONO (possible contaminant in the NO_2 beam). Kawasaki et al.[14] have shown that photodissociation of N_2O_4 at 193 and 248 nm gives rise to exclusively excited state NO_2 products and they did not find any evidence for NO or O formation.

An examination of the spectroscopy of the γ bands of NO shows that the (4,5) vibrational band has an origin at 225.6 nm. Thus various rotational lines from the (4,5) band can overlap with the (0,0) band which normally is thought to dominate in the 226 nm region. The Frank-Condon factors for the (4,5) and (0,0) bands are 0.057 and 0.162 respectively[15], but we have already seen that NO is formed predominantly in the v=5 level, so its contribution will show up clearly as we scan across the (0,0) band head of NO. This result shows that extracting rotational population distributions for NO (v=0) using the (0,0) transition is fraught with error if NO (v=5) is also formed in the process being examined. This overlapping of bands could account for the large NO (v=0) population observed by McFarlane et al. in the 248 nm photodissociation of NO_2, where they used 1+1 REMPI in the 224.9-227.5 nm region to obtain their NO (v=0) population.

It is apparent from the images shown for NO, that the angular distribution for the O(^3P) component is very different from the O(^1D) component. Fig.5 shows the angular distribution for O(^1D), derived from the Abel-transformed NO (v=0) images (the intense inner ring) shown in Fig.4(A) and (B). We derive a β of 0.6 ± 0.1 for NO (v=0) formed in conjunction with an excited state oxygen atom. For the NO(v=2) results shown in Fig.3(E) it is quite remarkable that the inner ring, corresponding to its formation in coincidence with O(^1D), is completely isotropic, while a nearby line (Fig. 3(F)) shows a strongly anisotropic angular distribution. The most likely explanation is simply that this level, so close to the energetic threshold for this process, experiences a long predissociation lifetime.

4 Discussion

Fig.6 shows the various energy levels for NO_2 that could be accessed with a 226 nm photon, and the energy levels for the dissociation pathways to O and

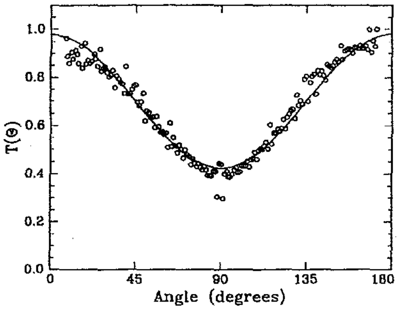

Figure 5: Angular distribution for inner ring of Fig. 3A: NO (v=0) formed in conjunction with O(^1D)

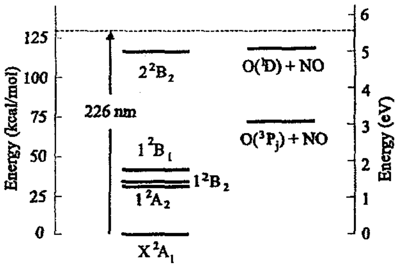

Figure 6: Schematic diagram showing the energy levels for the various relevant states of NO$_2$ and products.

NO. Most studies of NO$_2$ photodissociation have been performed near the threshold of the O(^3P_j) + NO channel where the NO$_2$ is primarily excited to the 1($^2B_2$) and/or 1($^2B_1$) electronic states. At 226 nm, in addition to these states, NO$_2$ can be excited to the 2($^2B_2$) state. A transition to this state is fully allowed from the X ($^2A_1$) ground state; this state is predissociative with a lifetime of about 42 ps at the origin, decreasing to the sub-picosecond regime by the first progression band[16].

Using chemical actinometry techniques, Uselman and Lee[17], showed that upon absorption of a 228.8 nm photon, NO$_2$ dissociated to form O(^1D) and O(^3P) in equal amounts. They postulated that above 245 nm, where the O(^1D) quantum yield was practically zero, case I predissociation[18] (nonradiative transition to the continuum of another electronic state) dominates. Below 245 nm, case II predissociation (dissociation by vibrational rearrangement to a vibrational manifold with a lower dissociation limit than the discrete vibrational manifold, both in the same electronic state) plus case I predissociation was operative. Uselman and Lee suggested that O(^3P) was formed by the case I and O(^1D) by case II mechanisms.

Rubahn et al.[7] carried out an extensive study on the fine-structure population distributions of O(^3P_J) from the photolysis of NO$_2$ over a range of wavelengths. Compared to 355 nm, they found that at 226 nm, the fine structure distributions had a propensity to populate the 1 and 0 levels. Miyawaki et al.[8] saw a similar effect for photodissociation at 212 nm. Both groups argued that the opening up of the O(^1D) + NO channel somehow affected the spin-orbit ratios for the ground state oxygen atom.

Since the ground state is totally symmetric ($^2A_1$), the transition dipole will have the same symmetry as the excited state. This means that the transition dipole moment will be perpendicular to the C_2 axis and in the plane of the molecule. Prompt dissociation from this geometry will give rise to β=1.4. For O($^3P_0$), we find β=1.3, and for the outer component in the various NO images we find similar anisotropy parameters. These results are consistent with prompt dissociation from the B($^2B_2$) state. Hradil et al.[19] report a value of 1.2 ± 0.3 for the O($^3P_2$) fragment formed in the 355 nm dissociation of NO_2 using photofragment ion imaging. The observation of a lower anisotropy parameter for the O(^1D) channel in our experiments is consistent with a case II predissociation where the transition state is longer lived compared to case I (the O(^3P) case). The observed angular distribution (the lower β parameter) for O(^1D) could also come from dissociation via a more strongly bent NO_2 excited state geometry.

An explanation for the different ratios for O(^1D):O(^3P) for various NO co-fragments is not forthcoming from the present results. Clearly more experiments should be performed in which separate lasers are used to initate the photodissociation of NO_2 and probe the NO photofragment. Finally experiments are underway to study the O(^1D) + NO channel directly, using REMPI to probe O(^1D) at 205 nm.

Acknowledgments
This work was supported by the Director, Office of Energy Research, Office of Basic Energy Sciences, Chemical Sciences Division of the U. S. Department of Energy under contract No. DE-ACO3-76SF00098.

References

[1] G.E. Busch and K.R. Wilson, J. Chem. Phys. **56**, 3626 (1972).

[2] S. A. Reid, D. C. Dobie, and H. Reisler, J. Chem. Phys. **100**, 4256 (1994).

[3] C.-H. Hsieh, Y.-S. Lee, A. Fujii, S.-H. Lee, and K. Liu, Chem. Phys. Lett. **277**, 33 (1997).

[4] T.G. Slanger, W.K. Bischel, and M.J. Dyer, J. Chem. Phys. **79**, 2231 (1983).

[5] J. McFarlane, J.C. Polanyi, and J.G. Shapter, J. Photochem. Photobiol. A: Chem. **58**, 139 (1991).

[6] L. Bigio, R.S. Tapper, and E.R. Grant, J. Phys. Chem. **88**, 1271 (1984).

[7] H. G. Rubahn, W.J. van der Zande, R. Zhang, M.J. Bronikowski, and R.N. Zare, Chem. Phys. Lett. **186**, 154 (1991).

[8] J. Miyawaki, T. Tsuchizawa, K. Yamanouchi, and S. Tsuchiya, Chem. Phys. Lett. **165**, 168 (1990).

[9] N. Shafer, K. Tonokura, Y. Matsumi, S. Tasaki, and M. Kawasaki, J. Chem. Phys. **95**, 6218 (1991).

[10] A.T.J.B. Eppink and D.H. Parker, Rev. Sci. Instr. **68**, 3477 (1997).

[11] M. Ahmed, D. A. Blunt, D. Chen, and A. G. Suits, J. Chem. Phys. **106**, 7617 (1997).

[12] D. Proch and T. Trickl, Rev. Sci. Inst. **60**, 713 (1989).

[13] M. Ahmed, D. S. Peterka, O. Vasyutinskii, A. S. Bracker, and A. G. Suits, Unpublished results .

[14] M. Kawasaki, K. Kasatani, , and H. Sato, Chem. Phys. **65**, 78 (1983).

[15] D. C. Jain and R. C. Sahni, Trans. Faraday Soc. **64**, 3169 (1968).

[16] K. E. J. Hallin and A. J. Merer, Can. J. Phys. **54**, 1157 (1976).

[17] W.M. Uselman and E.K.C. Lee, J. Chem. Phys. **65**, 1948 (1976).

[18] G. Herzberg, *Molecular Spectra and Molecular Structure III, Electronic Spectra and Electronic Structure of Polyatomic Molecules, 2nd Ed.*, Krieger, Coral Gables, Florida, 1991.

[19] V.P. Hradil, T. Suzuki, S. A. Hewitt, P.L. Houston, and B.J. Whitaker, J. Chem. Phys. **99**, 4455 (1993).